Editors' Suggestion

Correlated Double-Electron Additions at the Edge of a Two-Dimensional Electronic System

Ahmet Demir,[1] Neal Staley,[1] Samuel Aronson,[1] Spencer Tomarken,[1] Ken West,[2] Kirk Baldwin,[2] Loren Pfeiffer,[2] and Raymond Ashoori[1,*]

[1]Department of Physics, Massachusetts Institute of Technology, Cambridge, Massachusetts 02139, USA
[2]Department of Electrical Engineering, Princeton University, Princeton, New Jersey 08544, USA

(Received 26 January 2021; accepted 1 June 2021; published 23 June 2021)

We create laterally large and low-disorder GaAs quantum-well-based quantum dots that act as small two-dimensional electron systems. We monitor tunneling of single electrons to the dots by means of capacitance measurements and identify single-electron capacitance peaks in the addition spectrum from occupancies of one up to thousands of electrons. The data show two remarkable phenomena in the Landau level filling factor range $\nu = 2$ to $\nu = 5$ in selective probing of the edge states of the dot: (i) Coulomb blockade peaks arise from the entrance of two electrons rather than one; (ii) at and near $\nu = 5/2$ and at fixed gate voltage, these double-height peaks appear uniformly in a magnetic field with a flux periodicity of $h/2e$, but they group into pairs at other filling factors.

DOI: 10.1103/PhysRevLett.126.256802

Coulomb repulsion dictates an increase in the amount of energy required to add each successive electron to an isolated quantum dot, resulting in distinct electron additions in a periodic pattern known as a Coulomb blockade spectrum [1–6]. Such a uniform pattern is commonly seen in two-dimensional (2D) semiconductor quantum dots [6,7]. In contrast, in superconducting dots, Cooper pairing leads to deviations from ordinary Coulomb blockade, producing individual peaks in the addition spectrum that arise from the addition of two electrons [8–10]. The ground state of a superconducting island favors even numbers of electrons, resulting in parity-induced suppression of Coulomb blockade [11,12] and $2e$ tunneling.

Here, we present results from an experiment that, surprisingly, reveals $2e$ tunneling into edge states of large 2D semiconductor quantum dots. Remarkably, we observe that, in the vicinity of Landau level filling factor $5/2$, the electron additions to the edge states behave identically to the observed behavior for Cooper pairs entering a superconducting dot [8], with all electrons entering as pairs, with no additional energy cost for adding a second electron after the first. Moreover, the paired additions exist over a wide range of filling factors (from $\nu = 2$ to $\nu = 5$), but, at filling factors other than $5/2$, the double additions themselves group into pairs of double additions.

Laterally confined 2D quantum dots (QDs) provide a simple system to study confined electrons and their interactions [6,13–15]. However, conventional transport measurements on lateral quantum dots function by passing a current through them and can detect only delocalized electronic states [7], although recent rf techniques show sensitivity to localized charge pockets near the confining gates [16]. Here, we instead utilize a vertical tunneling geometry that eliminates lateral contacts and allows us to track electron additions to both localized and extended states starting from the first addition up to thousands of electrons over a wide range of magnetic field [4,17]. We have also developed a sample design to create quantum-well-based large QDs with very low disorder. The dot is confined between two electrodes in the "tunnel capacitor" structure shown schematically in Figs. 1(a) and 1(b). Unlike previous work, the structure does not contain any modulation doping [18] nor a Schottky barrier above the dot but instead requires the creation of a small Ohmic contact, comparable to the dot size, to the tunneling electrode above the dot. For this new design, we observe features associated with higher sample quality such as a considerably sharpened capacitance step upon adding charge to large QDs and the observed absence of states from silicon impurities in or near the QD [17].

We detect electron additions as peaks in the capacitance of this tunnel capacitor using a capacitance bridge technique in which we balance the QD against a known reference capacitor [17]. When a single electron tunnels from the tunnel electrode to the quantum dot, image charge accumulates on the opposite electrode. Using a low-temperature transistor charge amplifier, we read out the voltage created by this image charge to find the capacitance change [17]. The gate voltages for the observed capacitance directly reflect the ground state energies of the quantum dot containing different numbers of electrons [4,6,17]. Previously, these and other electron addition spectroscopy measurements of quantum dots showed well-defined transitions into the integer quantum Hall states [14,15,19,20].

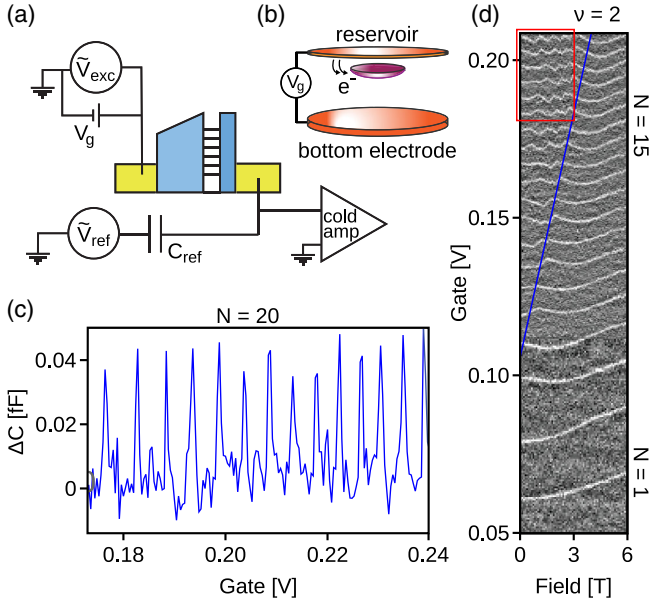

FIG. 1. Electron additions in a small 2D quantum dot. (a) The quantum dot is confined between two electrodes, one of which (tunneling electrode) is tunnel coupled to the dot. The carrier concentration can be tuned by the gate electrode. (b) Schematic of the sample design with a small metallic island (dot) that is tunnel coupled to a reservoir and capacitively coupled to the bottom electrode. (c) Isolated electron additions as a function of the gate voltage. The spacing between successive capacitance peaks largely reflects the additional energy required to overcome the Coulomb repulsion of the electrons already in the dot. The heights of the single-electron capacitance peaks in this trace are typical of those measured throughout the experiment. (d) Single-electron capacitance peaks (bright curves) in a small quantum dot as a function of the external magnetic field and gate voltage.

To illustrate the functioning of the capacitance method, we first show data in Figs. 1(c) and 1(d) from a small dot (∼120 nm) that does not show the pairing effect and follows standard "artificial atom" physics [6,13]. Electron additions occur periodically in gate voltage with a period of roughly e/C_g, where C_g is the capacitance between the gate and the dot. After each electron is added to the dot, adding a successive electron requires increased gate voltage due to Coulomb repulsion [2–5]. Figure 1(d) presents capacitance data taken from a small dot in a dilution refrigerator with a base temperature of 45 mK. These data show electron additions from $N = 1$ to $N = 20$ under an external perpendicular magnetic field, displaying features that fit with a model of a small quantum dot with a parabolic confining potential [21,22]. As the gate voltage is swept on the y axis, capacitance peaks appear for every electron that enters the dot. Note that the lateral extent of electrons in the dot gradually increases with the electron number, decreasing the observed spacing [4]. The blue line shows the density and field at which all electrons occupy spin-degenerate states belonging to the lowest orbital Landau level [$\nu = 2$ in a two-dimensional electron system (2DES)].

The "zigzags" in the evolution of the single-particle peaks with the magnetic field (red box in Fig. 1) indicate crossings of energies of single-particle states. As the magnetic field increases, the energies of the edge states move down relative to those of the bulk states, since their orbital magnetic moment is aligned with the field [6]. At the crossovers of different states, the descending energy of an electronic edge state falls below the ascending energy of a filled bulk state. Consequently, the peak position is expected to zig and zag as the highest-energy electron in the dot moves from one state to another. The zigzag behavior ends when all electrons fall into the lowest Landau level, at filling factor $\nu = 2$.

Increasing the dot area by an order of magnitude, we observe effectively quantum Hall physics in comparison to "artificial atom" physics [6,13] that we have shown in Fig. 1. For large dot sizes, self-consistent calculations [23,24] (see Supplemental Fig. S10 [25]) show that the electron density remains nearly uniform over most of the interior of the dot and diminishes only near the dot edges. Under the presence of an external magnetic field, electrons in the mini-2DES develop Landau levels. Figure 2 shows capacitance data from a large dot with a lithographic diameter of 800 nm. Figure 2(a) shows data from rastering the gate voltage scan and stepping through a wide range of magnetic fields and subtracting offsets from drifts in the measurement. Electrons start to populate the dot at around $V_{\text{gate}} = -0.1$V. In Fig. 2(a), the darker regions correspond to fully filled incompressible states, whereas the lighter regions correspond to partially filled compressible states. The data display a clear "Landau fan," indicated by black lines.

In Fig. 2(d), the first electron addition to the dot appears at −0.094 V at zero magnetic field. The positions of all electron addition peaks evolve with nearly zero slope at a small magnetic field. The slope increases with the field until the traces appear as nearly straight lines at high fields with slope $\hbar\omega_c/2B$ (where ω_c is the cyclotron frequency) as would be expected for spatially isolated localized states with a diamagnetic shift due to an applied magnetic field [17]. The data are taken with a small 200 μV rms excitation at 247 kHz, a frequency sufficiently lower than the tunneling rate so that the electrons tunnel in and out of the dot in phase with the applied excitation.

As more electrons are added to the dot, the charges from different localized states merge to create a single small "droplet" 2DES. As the droplet expands laterally, its capacitance to the surroundings increases, decreasing the charging energy for subsequent electron additions until we lose the ability to resolve individual capacitance peaks around zero B field.

Figure 2 shows two distinct groups of interaction-driven localized states that appear at filling factors $\nu = 1$ and

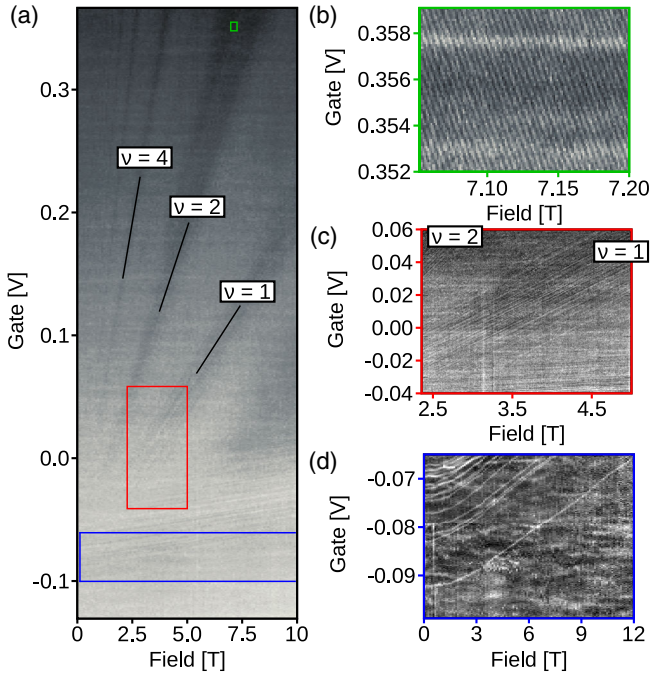

FIG. 2. Electron additions in a large quantum dot. Brighter regions correspond to higher capacitance. (a) Under a perpendicular magnetic field, the 2DES forms Landau levels, producing dips in the capacitance corresponding to each integer filling factor. There are roughly 2000 electron additions in the voltage range shown. (b) States with negative slope, corresponding to edge states, near $\nu = 5/2$. The broad horizontal lines may correspond to states under the gate region but outside of the dot itself. (c) Localized states in the Landau gap follow the underlying filling factor. States in the center and the top left of the figure track $\nu = 1$ and $\nu = 2$, respectively. The states that are nearly parallel to the field axis are the first few electrons added to the dot in isolated localized states, as in Ref. [26]. (d) Capacitance peaks of the first few electrons added to the dot as a function of the magnetic field.

$\nu = 2$. These localized states follow the slopes of the underlying Landau levels and appear only when the Landau level is fully filled. Screening of the electrostatic potential arising from disorder depends sensitively on the Landau level filling factor [23,27,28]; a partially filled level significantly screens the disorder potential, but, around integer ν, the electronic density of states is small and the disorder potential is poorly screened, leading to compressible charge pockets separated by incompressible barriers. In Fig. 2(c), the peaks that run parallel to integer ν arise from electron additions to these pockets [23,26,29].

Similar peaks appear around every well-developed integer quantum Hall state as also appeared in previous work studying a 2DES gated by a local scanning single-electron transistor [26]. The charging peaks in that work arose from electrons moving laterally within a very large 2DES to fill individual localized compressible islands in an otherwise incompressible region. In contrast, charge quantization always occurs in our lithographically defined quantum dots, allowing us to observe single-electron additions into both compressible and incompressible regimes. This capability led us to observe a remarkable series of periodic electron additions that appear in the compressible regions.

We now focus on performing fine measurements in compressible regions with very large numbers (~2000) of electrons in the dot. In Fig. 2(b), we observe states that are evenly spaced in the magnetic field. Unlike the electron additions in a small quantum dot [Fig. 1(d)], where the electron addition peaks show zigzags, the spectra show only uniform straight lines. The energies of these states all move down with an increasing magnetic field, as would be expected only for electronic states at the edge of the mini-2DES [6]. This highly uniform spacing and downward movement of all observed states suggest that the edge of the 2DES remains "compact," with all angular momentum states filled. This is the situation that is sometimes expected at filling factor $\nu = 1$ [14,20,30] in a "maximum density droplet" [30] (MDD) with no "edge state reconstructions" [31] occurring in the range of these datasets. In the case of such a $\nu = 1$ MDD, one would expect a single-electron addition for each additional magnetic flux quantum h/e threading the dot. We note that our data at these densities and filling factors do not display all electron additions to the dot. In a large-area 2D electron system, tunneling from a 3D electrode into the bulk of the 2D system is suppressed exponentially by a magnetic-field-induced Coulomb gap [32,33]. In contrast, there is only power-law suppression for tunneling into edge states [34], and electrons tunneling to the edge still do so at short timescales compared to the inverse frequencies of the ac excitations in our measurements. At fixed gate bias, electrons enter the dot as we increase the magnetic field, but charge balance can be maintained as electrons not visible to the experiment tunnel out of the center of the dot to the tunneling electrode (see Supplemental Material [25] for simulations showing the small variation of the total number of electrons in the dot with a varying magnetic field).

In Fig. 3, we plot the comparison between the edge states near $\nu = 3/2$ and those near $\nu = 5/2$. Edge state lines correspond to constant flux, with one flux quantum difference between each constant flux line. The periodicity of electron peaks in the field and gate voltage is halved at $\nu = 5/2$ as compared to $\nu = 3/2$. To illustrate this, we performed Fourier analysis of two regions, plotted in Fig. 3(c). The periodicity in the magnetic field when the filling factor is $\nu < 2$ (blue curve) is $\Delta B = 13$ mT. This yields a dot area of 0.55 μm^2, close to what is expected in our simulations (see Supplemental Fig. S10 [25]). However, when the filling factor is tuned to near $\nu = 5/2$ (red curve), we observe a doubling of the electron peak frequency compared to the situation at $\nu = 3/2$.

In capacitance measurements, the capacitance peak height reflects the amount of tunneling charge [17]. In Fig. 4(a), we compare the peaks of isolated first electrons

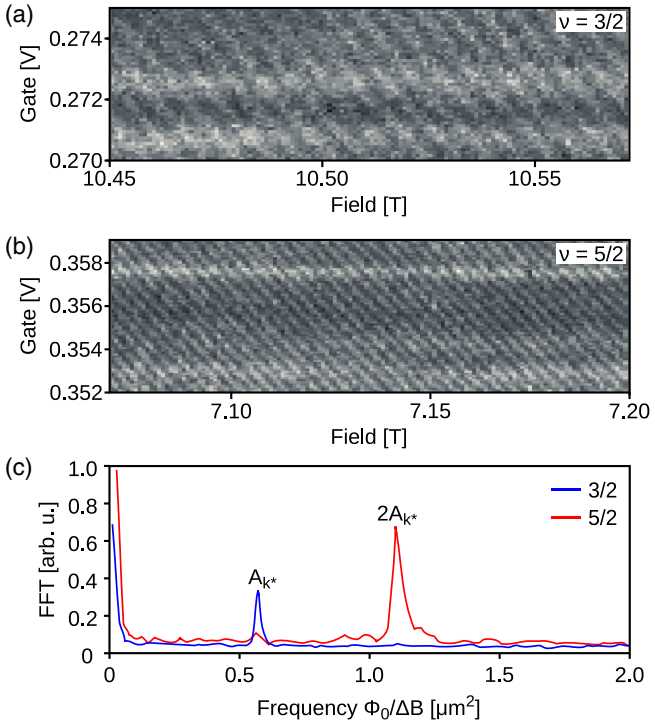

FIG. 3. Electron addition spectra in the $N = 0$ versus the $N = 1$ Landau level. (a) Capacitance data taken as a function of the gate voltage and magnetic field in the $\Phi_0 = h/e$ regime. The filling factor is near $\nu = 3/2$. (b) When the gate voltage is tuned to near filling factor $\nu = 5/2$, the periodicity in the magnetic field is halved. (c) Corresponding Fourier transforms of two different regions as a function of $\Phi_0/\Delta B$. The blue and red curves are the Fourier transforms near $\nu = 3/2$ and $\nu = 5/2$, respectively.

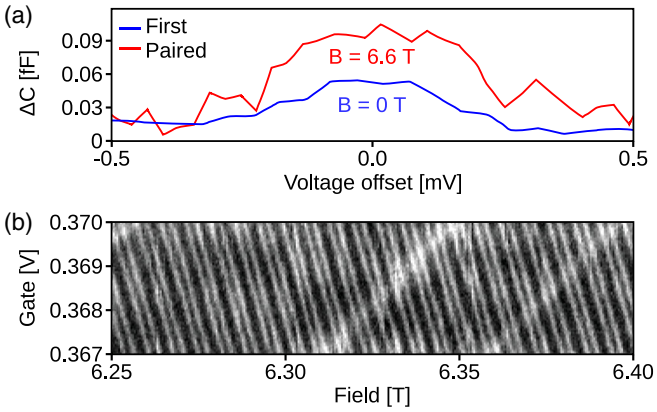

FIG. 4. Double-height peaks in the $N = 1$ Landau level and bunching of paired peaks away from filling factor $\nu = 5/2$. (a) Electron charge comparison between the first electrons and the paired electrons. The blue curve (first electrons) is centered at a bias voltage of -0.0795 V and the red curve (paired electrons) at 0.3655 V. (b) High magnetic field resolution measurement showing bunched pairs. The ac excitation is 100 μV rms. The filling factor ranges from $\nu = 2.9$ at 6.25 T to $\nu = 2.83$ at 6.40 T. As this scan is close to $\nu = 3$, notice that two localized states appear with positive slope. However, the localized states do not appear to interact with the edge states at all.

(blue curve) to those of edge states near filling factor $\nu = 5/2$ (red curve) and find, remarkably, that they arise from the charge of two electrons tunneling back and forth across the barrier (see Supplemental Material [25]). These double-electron additions contradict the prediction of Coulomb blockade theory [2,3,5] that more energy is required to add each successive electron to a quantum dot as a result of electron repulsion. While prior measurements on more disordered dots at lower densities also showed a violation of Coulomb blockade with pairing and bunching of electron addition peaks [17,19,35,36], the current results differ in that *all* observed electron additions, over nearly the entire range of ν between integer values of ν, occur as pairs. They thus appear more similar to pairing phenomena observed in charging superconducting islands [8–10], where ground states of even and odd numbers of electrons have energies differing by the superconducting gap, resulting in parity-induced suppression of Coulomb blockade [11,12].

Another surprising observation is that the double-electron peaks themselves bunch together at all filling factors between $\nu = 2$ and $\nu = 5$ with the only clear exception at $\nu = 5/2$, where the peaks are evenly spaced. Beyond $\nu = 5$, the peaks become difficult to discern. Figure 4(b) demonstrates this bunching, presenting data taken with a 100 μV rms excitation. In Fig. S8 [25], we provide data similar to that shown in Fig. 4(b) but over a broad filling factor range including $\nu = 5/2$. Similar behaviors, such as the $h/2e$ periodicity, bunching phenomena, and localized states, all occur in another dot with a lithographic area of 0.325 μm^2.

Our results may have a connection to a different type of experiment [37,38] performed on a Fabry-Perot interferometer (FPI) fabricated on a 2DES confined by two quantum point contacts. Allowing only the outermost edge channel through the quantum point contacts, the FPI should show oscillations of period h/e for single-electron orbits. The FPI experiment displays this predicted behavior between filling factors $\nu = 1$ and $\nu = 2$, but the periodicity in the magnetic field is halved between $\nu = 5/2$ and $\nu = 5$, yielding $h/2e$ oscillations (in contrast with $2e$ flux quantum between $\nu = 2$ and $\nu = 5$ in our experiment), with quantum shot noise measurements also suggesting a quasiparticle charge of $2e$ rather than e [37]. Shot noise measurements result from out-of-equilibrium tunneling events, but the two-electron additions in our experiment, existing in the limit of small excitation drive, take place in thermodynamic equilibrium. Moreover, while the FPI data reveal a mechanism that binds two electrons together as they encircle the FPI, our results now show that the energetics of this binding is sufficiently strong to produce violation of Coulomb blockade. Finally, our data (see Supplemental Material and Figs. S8 and S9 [25]) appear to demonstrate that each of the two electrons in a pairing enters a single edge state, and alternate pairs in a two-pair bunch enter different edge states.

The observed tunneling into the edge states shows no sign of decreased tunneling rate that would appear as phase shifts in the charging response. "Negative-U" models, involving sequential tunneling and rearrangements of the electronic system in the bulk [39,40] or at the edge [41] of a 2D system, place two peaks at the same gate voltage. However, such models would result in diminished tunneling rates in our experiment. To have two electrons tunneling back and forth between the dot and the tunneling electrode at the exact same gate voltage, the first electron in a pair must first tunnel into the dot with less than the required energy ΔE to produce the rearrangement. Therefore, the second electron in the pair must tunnel into the dot at a rate that is fast compared to $\Delta E/\hbar$ ($\sim 10^{11}$ s^{-1} for the $\approx$0.4 meV energy barrier as seen from the gate voltage spacing of single-electron peaks). As tunneling rates in our dots from the tunneling electrode are on the order of 10^6 s^{-1}, such negative-U models cannot explain our data. Another possibility would then be an effective zero repulsion between electrons in a pair, but we know of no model for this. The answer may lie in coherent tunneling of the two electrons. For instance, in tunneling to superconducting islands from a normal metal electrode [10], the tunneling rate is enhanced due to Andreev processes compared with the suppressed incoherent tunneling of two electrons [12]. Indeed, the occupancy of uniform (unbunched) pairs occurring only very near $\nu = 5/2$ may suggest that such coherent tunneling could have a connection with the $5/2$ fractional quantum Hall state, where theory describes a potential Cooper pairing of composite fermions [42]. As discussed in Supplemental Material [25], more sophisticated time-domain pulsed capacitance measurements [43] could provide further information regarding the microscopic origins of the observed pairing and bunching effects.

Measurement and analysis of quantum dot data were carried out with support from Basic Energy Sciences Program of the Office of Science of the U.S. Department of Energy, Contract No. FG02-08ER46514. Fabrication of the quantum dots was performed at MIT Microsystems Technology Laboratory with support from the Gordon and Betty Moore Foundation, through Grant No. GBMF2931, and the STC Center for Integrated Quantum Materials, National Science Foundation Grant No. DMR-1231319. S. A. was supported by the National Science Foundation Graduate Research Fellowship under Grant No. 1122374. We thank L. Levitov, P. A. Lee, and L. Glazman for helpful discussions.

*ashoori@mit.edu

[1] L. I. Glazman and R. I. Shekhter, Coulomb oscillations of the conductance in a laterally confined heterostructure, J. Phys. Condens. Matter **1**, 5811 (1989).
[2] C. W. J. Beenakker, Theory of Coulomb-blockade oscillations in the conductance of a quantum dot, Phys. Rev. B **44**, 1646 (1991).
[3] R. H. Silsbee and R. C. Ashoori, Comment on Zeeman Bifurcation of Quantum-Dot Spectra, Phys. Rev. Lett. **64**, 1991 (1990).
[4] R. C. Ashoori, H. L. Stormer, J. S. Weiner, L. N. Pfeiffer, K. W. Baldwin, and K. W. West, N-Electron Ground State Energies of a Quantum Dot in Magnetic Field, Phys. Rev. Lett. **71**, 613 (1993).
[5] M. H. Devoret and H. Grabert, Introduction to single charge tunneling, in *Single Charge Tunneling: Coulomb Blockade Phenomena in Nanostructures*, NATO ASI Series, edited by H. Grabert and M. H. Devoret (Springer US, Boston, MA, 1992), pp. 1–19.
[6] R. C. Ashoori, Electrons in artificial atoms, Nature (London) **379**, 413 (1996).
[7] M. A. Kastner, Artificial atoms, Phys. Today **46**, No. 1, 24 (1993).
[8] P. Lafarge, P. Joyez, D. Esteve, C. Urbina, and M. H. Devoret, Two-electron quantization of the charge on a superconductor, Nature (London) **365**, 422 (1993).
[9] M. T. Tuominen, J. M. Hergenrother, T. S. Tighe, and M. Tinkham, Experimental Evidence for Parity-Based 2e Periodicity in a Superconducting Single-Electron Tunneling Transistor, Phys. Rev. Lett. **69**, 1997 (1992).
[10] P. Joyez, P. Lafarge, A. Filipe, D. Esteve, and M. H. Devoret, Observation of Parity-Induced Suppression of Josephson Tunneling in the Superconducting Single Electron Transistor, Phys. Rev. Lett. **72**, 2458 (1994).
[11] K. A. Matveev, M. Gisselfalt, L. I. Glazman, M. Jonson, and R. I. Shekhter, Parity-Induced Suppression of the Coulomb Blockade of Josephson Tunneling, Phys. Rev. Lett. **70**, 2940 (1993).
[12] F. W. J. Hekking, L. I. Glazman, K. A. Matveev, and R. I. Shekhter, Coulomb Blockade of Two-Electron Tunneling, Phys. Rev. Lett. **70**, 4138 (1993).
[13] L. Kouwenhoven and C. Marcus, Quantum dots, Phys. World **11**, 35 (1998).
[14] T. H. Oosterkamp, J. W. Janssen, L. P. Kouwenhoven, D. G. Austing, T. Honda, and S. Tarucha, Maximum-Density Droplet and Charge Redistributions in Quantum Dots at High Magnetic Fields, Phys. Rev. Lett. **82**, 2931 (1999).
[15] S. Tarucha, D. G. Austing, T. Honda, R. J. van der Hage, and L. P. Kouwenhoven, Shell Filling and Spin Effects in a Few Electron Quantum Dot, Phys. Rev. Lett. **77**, 3613 (1996).
[16] X. G. Croot, S. J. Pauka, M. C. Jarratt, H. Lu, A. C. Gossard, J. D. Watson, G. C. Gardner, S. Fallahi, M. J. Manfra, and D. J. Reilly, Gate-Sensing Charge Pockets in the Semiconductor-Qubit Environment, Phys. Rev. Applied **11**, 064027 (2019).
[17] R. C. Ashoori, H. L. Stormer, J. S. Weiner, L. N. Pfeiffer, S. J. Pearton, K. W. Baldwin, and K. W. West, Single-Electron Capacitance Spectroscopy of Discrete Quantum Levels, Phys. Rev. Lett. **68**, 3088 (1992).
[18] R. Dingle, H. L. Störmer, A. C. Gossard, and W. Wiegmann, Electron mobilities in modulation-doped semiconductor heterojunction superlattices, Appl. Phys. Lett. **33**, 665 (1978).

[19] N. B. Zhitenev, M. Brodsky, R. C. Ashoori, L. N. Pfeiffer, and K. W. West, Localization-delocalization transition in quantum dots, Science **285**, 715 (1999).
[20] O. Klein, C. de C. Chamon, D. Tang, D. M. Abusch-Magder, U. Meirav, X. G. Wen, M. A. Kastner, and S. J. Wind, Exchange Effects in an Artificial Atom at High Magnetic Fields, Phys. Rev. Lett. **74**, 785 (1995).
[21] V. Fock, Bemerkung zur Quantelung des harmonischen Oszillators im Magnetfeld, Z. Phys. **47**, 446 (1928).
[22] C. G. Darwin, The diamagnetism of the free electron, Math. Proc. Cambridge Philos. Soc. **27**, 86 (1931).
[23] D. B. Chklovskii, B. I. Shklovskii, and L. I. Glazman, Electrostatics of edge channels, Phys. Rev. B **46**, 4026 (1992).
[24] M. M. Fogler, E. I. Levin, and B. I. Shklovskii, Chemical potential and magnetization of a Coulomb island, Phys. Rev. B **49**, 13767 (1994).
[25] See Supplemental Material at http://link.aps.org/supplemental/10.1103/PhysRevLett.126.256802 for device fabrication details, additional capacitance measurements, and simulations.
[26] S. Ilani, J. Martin, E. Teitelbaum, J. H. Smet, D. Mahalu, V. Umansky, and A. Yacoby, The microscopic nature of localization in the quantum Hall effect, Nature (London) **427**, 328 (2004).
[27] A. L. Efros, Non-linear screening and the background density of 2 deg states in magnetic field, Solid State Commun. **67**, 1019 (1988).
[28] D. G. Polyakov and B. I. Shklovskii, Activated Conductivity in the Quantum Hall Effect, Phys. Rev. Lett. **73**, 1150 (1994).
[29] N. R. Cooper and J. T. Chalker, Coulomb interactions and the integer quantum Hall effect: Screening and transport, Phys. Rev. B **48**, 4530 (1993).
[30] A. H. MacDonald, S.-R. E. Yang, and M. D. Johnson, Quantum dots in strong magnetic fields: Stability criteria for the maximum density droplet, Aust. J. Phys. **46**, 345 (1993).
[31] C. de C. Chamon and X. G. Wen, Sharp and smooth boundaries of quantum Hall liquids, Phys. Rev. B **49**, 8227 (1994).
[32] R. C. Ashoori, J. A. Lebens, N. P. Bigelow, and R. H. Silsbee, Equilibrium Tunneling From the 2-Dimensional Electron-Gas in GaAs—Evidence For a Magnetic-Field-Induced Energy-Gap, Phys. Rev. Lett. **64**, 681 (1990).
[33] R. C. Ashoori, J. A. Lebens, N. P. Bigelow, and R. H. Silsbee, Energy gaps of the two-dimensional electron gas explored with equilibrium tunneling spectroscopy, Phys. Rev. B **48**, 4616 (1993).
[34] A. M. Chang, Chiral Luttinger liquids at the fractional quantum Hall edge, Rev. Mod. Phys. **75**, 1449 (2003).
[35] N. B. Zhitenev, R. C. Ashoori, L. N. Pfeiffer, and K. W. West, Periodic and Aperiodic Bunching in the Addition Spectra of Quantum Dots, Phys. Rev. Lett. **79**, 2308 (1997).
[36] M. Brodsky, N. B. Zhitenev, R. C. Ashoori, L. N. Pfeiffer, and K. W. West, Localization in Artificial Disorder: Two Coupled Quantum Dots, Phys. Rev. Lett. **85**, 2356 (2000).
[37] H. K. Choi, I. Sivan, A. Rosenblatt, M. Heiblum, V. Umansky, and D. Mahalu, Robust electron pairing in the integer quantum Hall effect regime, Nat. Commun. **6**, 1 (2015).
[38] I. Sivan, R. Bhattacharyya, H. K. Choi, M. Heiblum, D. E. Feldman, D. Mahalu, and V. Umansky, Interaction-induced interference in the integer quantum Hall effect, Phys. Rev. B **97**, 125405 (2018).
[39] M. E. Raikh, L. I. Glazman, and L. E. Zhukov, Two-Electron State in a Disordered 2d Island: Pairing Caused by the Coulomb Repulsion, Phys. Rev. Lett. **77**, 1354 (1996).
[40] A. Hamo, A. Benyamini, I. Shapir, I. Khivrich, J. Waissman, K. Kaasbjerg, Y. Oreg, F. von Oppen, and S. Ilani, Electron attraction mediated by Coulomb repulsion, Nature (London) **535**, 395 (2016).
[41] A. A. Koulakov and B. I. Shklovskii, Charging spectrum and configurations of a Wigner crystal island, Phys. Rev. B **57**, 2352 (1998).
[42] V. W. Scarola, K. Park, and J. K. Jain, Cooper instability of composite fermions, Nature (London) **406**, 863 (2000).
[43] O. E. Dial, R. C. Ashoori, L. N. Pfeiffer, and K. W. West, High-resolution spectroscopy of two-dimensional electron systems, Nature (London) **448**, 176 (2007).